

Article

Mechanical Degradation and Thermal Decomposition of Ethylene-Vinyl Acetate (EVA) Polymer-Modified Cement Mortar (PCM) Exposed to High-Temperature

Hyung-Jun Kim ¹, Jae-Yeon Park ², Heong-Won Suh ², Beom-Yeon Cho ³, Won-Jun Park ⁴ and Sung-Chul Bae ^{2,*} 

¹ Hazard Mitigation Evaluation Technology Center, Korea Conformity Laboratories, Cheongju 28115, Korea; arc7707@kcl.re.kr

² Department of Architectural Engineering, Hanyang University, Seoul 04763, Korea; p9206@naver.com (J.-Y.P.); christ1205@naver.com (H.-W.S.)

³ Korea Institute of Civil Engineering and Building Technology, Gyeonggi-do 10223, Korea; choby277@kict.re.kr

⁴ Department of Architectural Engineering, Kangwon National University, Samcheok 25913, Korea; wjpark@kangwon.ac.kr

* Correspondence: sbae@hanyang.ac.kr; Tel.: +82-2-2220-0302

Received: 14 December 2018; Accepted: 17 January 2019; Published: 18 January 2019



Abstract: A polymer-modified cement mortar (PCM) is widely used as a repair material for reinforced concrete (RC) structures owing to its excellent strength and durability. However, considering the maintenance of the RC structures and the use period of the structures, the change in the physical properties of the PCM should be evaluated when exposed to various high-temperature environments, such as fires. In this study, the degradation of the mechanical properties (compressive strength and modulus of elasticity), thermal decomposition of the PCM in various high-temperature environments, and the change in the pore structure of the PCM after exposure to high temperatures were quantitatively investigated. A mechanical property evaluation of PCM was performed under three heating conditions: (i) heating in a compression tester, (ii) heating the specimen in an oven to a predetermined temperature and then moving it to a compression tester preheated to the same temperature, and (iii) cooling to room temperature after heating. In the experiment, a PCM specimen was prepared by changing the polymer–cement ratio (polymer content) of ethylene-vinyl acetate (EVA), the most commonly used polymer, to perform a high-temperature sectional test from 200 to 800 °C. In addition, to investigate the change in the PCM mechanical properties in the high-temperature region, in terms of the pyrolysis of EVA, the porosity change and mass change were examined using thermal analysis and mercury intrusion porosimetry. Before heating, the compressive strength of the PCM increased with the EVA content up to 10 % of the polymer–cement ratio. Under the cooling conditions after heating up to 200 °C, the mechanical performance of the PCM was restored, whereas the degradation of the mechanical properties of the PCM without cooling was more pronounced. Furthermore, the mass loss, heat flow, and the total porosity of the PCM increased as the EVA content increased, which is correlated with the degradation of the mechanical properties of the PCM.

Keywords: polymer-modified cement mortar; ethylene-vinyl acetate; mechanical properties; repair materials; heating

1. Introduction

Polymer-modified cement mortar (PCM) is superior to ordinary cement mortar in terms of strength, durability, chemical resistance, and workability and is widely used for repairing and strengthening reinforced concrete (RC) structures [1–4]. In earlier studies, PCM has shown different physical and mechanical properties than those of ordinary inorganic cement mortar and concrete because PCM is a mixture of polymeric organic material and cement mortar [5–7]. Considering the maintenance of RC buildings and the use period of the structures, the change in the physical properties of the PCM when exposed to high-temperature environments, such as fires, should be evaluated [8,9].

However, currently, studies on the mechanical properties of PCM exposed to high-temperature environments and experiments on PCM before and after exposure to high temperatures are insufficient [10–12]. It is due to the difficulties to obtain sufficient experimental data on the PCM mechanical properties at high temperatures, as the evaluation (compression test) in a high-temperature environment (or during a fire) requires a long preparation time, expensive measuring equipment, heating, and temperature control for each high-temperature region [10–13]. Moreover, there is a risk that the test equipment may be damaged if spalling occurs during heating in a state where the test object is completely shut off. Therefore, an easier method to evaluate the mechanical characteristics of the PCM in a high-temperature environment is required.

Conversely, concrete, which is an inorganic material, is known to undergo mechanical property changes depending on the heating temperature range. Its compressive strength is reduced at 100 °C and recovers to near room temperature strength at 200 °C. The strength decreases at a temperature range of 450–550 °C, at which calcium hydroxide, which is the main hydration product of cement clinkers C_3S (tricalcium silicate) and C_2S (dicalcium silicate), decomposes in the section exceeding 300 °C [14–16]. The reason for the decrease in the compressive strength at 100 °C is the expansion of the aggregate and the contraction and stress in the cement hydrate owing to water evaporation inside the concrete. The change in the compressive strength at 100–300 °C is attributed to complicated causes, such as the difference in the thermal expansion and the deformation of different constituents of the concrete and the acceleration of the hydration of the untreated cement clinker particles owing to the moisture evaporating at a high-temperature in the concrete [14,17].

For PCM-applied concrete, the relationship between the compressive strength and temperature under heating and cooling-after-heating, for concrete with the same materials and composition, is summarized as follows [13]. The compressive strength for regular concrete decreases when heating to 100 °C and increases again between 200 and 300 °C. Thereafter, as the temperature increases, the compressive strength gradually decreases and then sharply decreases at 400 °C or higher. However, because the effect of the thermal decomposition of the polymer and the origin of the high-temperature characteristics of ordinary concrete must be considered for PCM, a more complex analysis of the effects of pyrolysis of the polymer (mass and porosity) is required, along with an empirical assessment of the expected fire resistance and yield strength degradation of the PCM used in concrete structure repair. Moreover, although PCM is widely used as a repair material for reinforced concrete structures, when PCM is burned, that is, when it is exposed to a high temperature owing to a fire in buildings that are repaired using PCM, spallation and ignition from the thermal decomposition of the polymer occur and the strength of the structure is expected to decrease [11–13,18]. Therefore, to understand the change in the mechanical properties of the PCM in high-temperature environments, in terms of the reuse of the PCM-applied structures after a fire, the mechanical properties of PCM should be understood in addition to the evaluated mechanical properties of the PCM under high-temperature conditions similar to the actual fire environment [19].

Therefore, in this study, the mechanical performance (compressive strength and elastic modulus) of the PCM at high temperatures, thermal decomposition, and the variation in the pore structure of the PCM after exposure to high temperatures were experimentally evaluated. PCM test specimens, in which the ethylene-vinyl acetate (EVA) content was varied in the polymer–cement ratio (EVA polymer incorporation amount), were prepared using two heating processes to carry out per-section

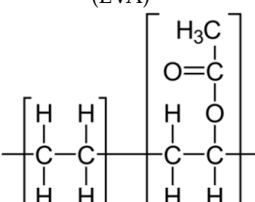
experiments between 200 and 800 °C: (i) heating in the compression tester and (ii) heating the specimen in the oven to the specified temperature and then moving it to a preheated compression tester. The specimens were compared to a specimen that was cooled to room temperature after heating. Through this study, the relationships between the compressive strength, modulus of elasticity, mass changes owing to the thermal decompositions, and pore structure of the PCM at various temperature ranges for different heating conditions were experimentally investigated.

2. Experiment Overview

2.1. Materials and Compositions

The types and properties of the polymers used in the experiments are listed in Table 1. EVA was used as the polymer, as standardized in the Japanese Industrial Standards (JIS) A 6203 (polymer dispersions and re-dispersible polymer powders for cement modifiers). The mixing ratios of the PCM specimens are listed in Table 2 [11,12]. The water–cement ratio of the PCM specimens was 50%, and the polymer–cement ratios were 0, 5, 10, and 20%. In terms of cement, Type I ordinary Portland cement specified in JIS R 5210 was used in addition to fine aggregate (fineness modulus 2.97, density 2.63 g/cm³, and water absorption 1.81%) specified in JIS A 5308 [20,21]. The chemical composition of the cement was determined via X-ray fluorescence spectroscopy (XRF, ZSX Primus II, Rigaku, Tokyo, Japan) as presented in Table 3. Meanwhile, 1% of a blowing agent was added in order to disperse the polymer powders in the PCM. The cement-fine aggregate ratio (weight ratio) was 1:3, and three specimens at each level were fabricated and tested. In this study, the amount of the polymer was expressed as weight per unit volume. For example, 10 kg/m³ of the unit polymer weight in the PCM composition corresponded to a 2% polymer–cement ratio.

Table 1. Properties of the polymer (EVA).

Type and Structure of the Polymer	Volatile Portion (%)	Residual Mass Ratio of Particle * (%)	Acid Value (mg KOH/mg)	Apparent Density (g/mL)
Ethylene-vinyl acetate (EVA) 	Less than 2.0	Less than 2.0	Less than 2.0	0.50 ± 0.10

* Residual mass ratio after passing through a 300 µm sieve.

Table 2. Mix proportions of the PCM specimens.

Type of Polymer	Specimens	Polymer–Cement Ratio (P/C) (%)	Water–Cement Ratio (W/C)	Water–Binder Ratio (W/B)
None	E0	0	0.5	0.5
	E5	5	0.53	
EVA	E10	10	0.56	0.5
	E20	20	0.63	

Table 3. Chemical compositions of ordinary Portland cement, as measured by XRF.

Composition (wt%)	SiO ₂	Al ₂ O ₃	Fe ₂ O ₃	CaO	MgO	K ₂ O	SO ₃	TiO ₂	LOI	Total
	18.42	2.84	2.16	68.18	2.35	1.13	3.01	0.15	1.76	100

2.2. Heating Conditions and Test Method

The PCM specimens for the mechanical test were manufactured with a dimension of $\phi 100 \times 200$ mm. After mixing the raw materials, the air content and the slump flow of the fresh PCM were measured. The specimens were wet-cured for 2 days (20 °C, 90% RH) and then underwater-cured at 20 °C for 28 days. After curing in water, aerial curing was carried out for 63 days under an environment of 20 °C and 60% RH. The specimens were dried in a drying furnace at 60 °C for one week before the heating test and then cooled to room temperature in a desiccator. Through these steps, the water absorption of the specimen was adjusted to within the range of 1.5 to 2.0% [22,23]. The curing procedure described above was accessed in accordance with JIS A 1171 (test methods for polymer-modified mortar).

Conversely, the appropriate heating rate should be determined to prevent spalling or an explosion owing to the thermal stress caused by the temperature difference between the center and surface of the specimen. In one of the preliminary experiments (the water content of the test body was approximately 3.0%), when the heating rate was 150 °C/h, the specimen spalled 3 h after heating; however, the specimen did not spall when the heating rate was 100 °C/h. Based on the results of the preliminary test, the water content of the test specimen was maintained below 2.0%, considering the two high-temperature environments and the heating program, as shown in Figure 1, was set at a heating rate of 100 °C/h [11–13]. To monitor the temperature at the center and surface of the specimen, a thermocouple was pre-embedded in the specimen, as shown in Figure 2a.

In the conventional compression test under heating, as shown in Figure 2b, a compression test was conducted after heating with the heater installed; however, there were issues with this test, such as a restriction of the number of experiments and equipment damage [13]. In this study, a specimen that reached a predetermined temperature during heating in the oven (Figure 2c) was transferred to a compression tester (Figure 2d) preheated to the same temperature and compressed. As a comparison, the sample heated until the internal temperature of the sample reached a predetermined temperature, as shown in Figure 1, and then the sample cooled in air was tested on the compressive machine.

In this study, (i) heating in a compression tester, (ii) heating the specimen in an oven to a predetermined temperature and then moving it to a compression tester preheated to the same temperature, and (iii) cooling to room temperature after heating were referred to as (i) in situ-heating, (ii) oven-heating, and (iii) cooling, respectively. Meanwhile, in the compression test during in situ- and oven-heating, the heating temperature was maintained for 0.5 to 2.5 h until the internal temperature of the test specimen reached the set temperature.

Pyrolysis of the PCM occurs in a high-temperature environment to generate gas, and most of the generated gas is released to the exterior of the test body; however, some of it is trapped in the pore structure inside the test body. The total amount of porosity and pore distribution were measured using mercury intrusion porosimetry (MIP, AutoPore IV, Micromeritics, Norcross, GA, USA). Moreover, the mass change and heat flow of EVA and PCM was measured by thermogravimetry (TG, heating rate: 20 °C/min, STA7200, Hitachi, Japan) and differential scanning calorimetry (DSC, heating rate: 20 °C/min, DSC7020, Hitachi, Tokyo, Japan). For the tests, the PCM specimen with dimension of 100 × 100 × 400 mm was prepared. The specimen was cured using the same protocol of the specimen for the mechanical test. After the curing, the specimen was sliced (100 × 100 × 10 mm) and dried in a drying furnace at 60 °C to control the water absorption of the specimen within the range of 1.5 to 2.0%.

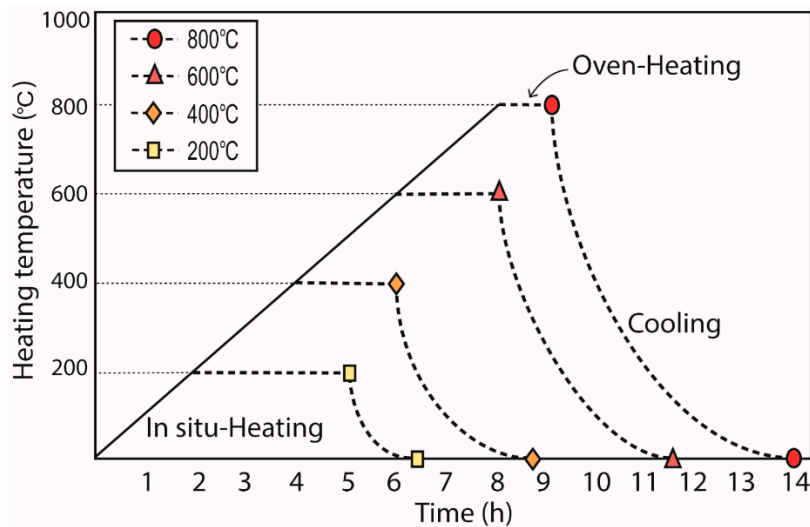


Figure 1. Heating program for the PCM specimens (in situ-heating, oven-heating, and cooling).

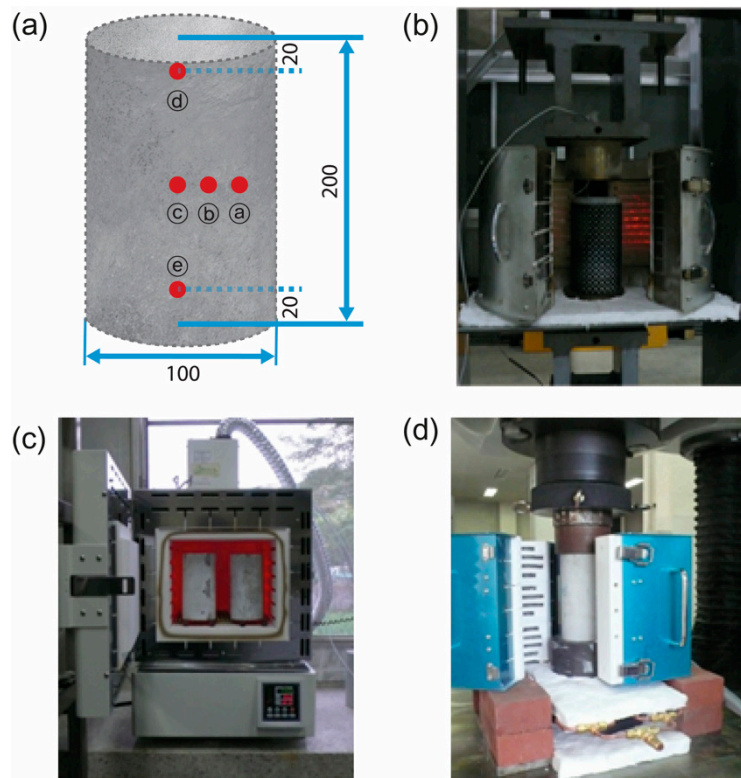


Figure 2. Setup for the compression test: (a) specimen dimension and the location of the thermocouple installation (unit: mm), (b) compressive strength test machine (in situ-heating) (previously used in [13]), (c) heating oven (oven-heating), and (d) compressive strength test machine (oven-heating).

3. Experimental Results and Analysis

3.1. Mechanical Properties of the PCM at Room Temperature (before Heating)

Figure 3 shows the compressive strength and modulus of elasticity of the PCM specimens with different mixing ratios of EVA at room temperature (unheated). The compressive strength of the PCM increased with the EVA content up to 10% of the polymer–cement ratio; however, the compressive strength slightly decreased when the ratio was increased to 20%. Similar to the compressive strength,

the modulus of elasticity of the PCM mixed with EVA increased for the 10% polymer–cement ratio and decreased for 20% incorporation.

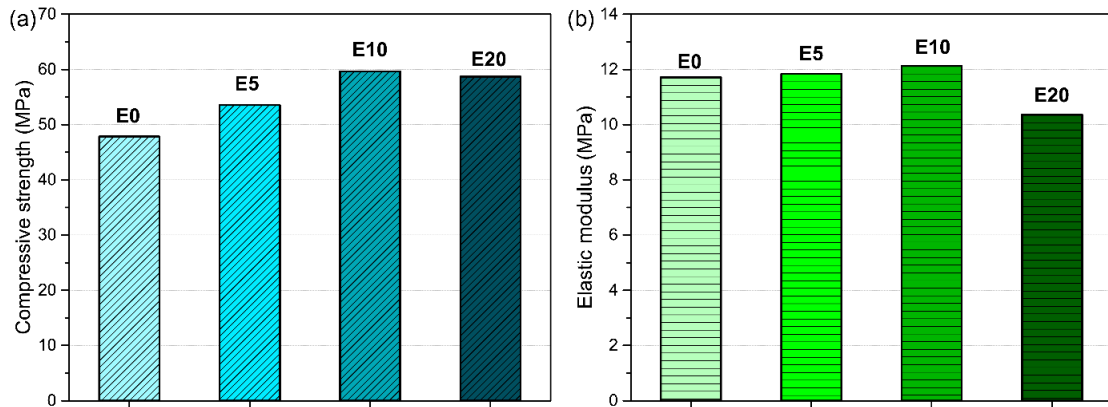


Figure 3. Mechanical properties of the PCM (unheated specimen): (a) compressive strength and (b) elastic modulus.

3.2. Preliminary Review of the Heating Methods (In Situ-Heating vs. Oven-Heating)

Unlike the existing in situ-heating methods, the oven-heating method requires the movement of a large number of test specimens from the preheating oven to the compressive test apparatus and the temperature of the test specimen may drop when the specimen is moved into the test machine from the preheating oven. Figure 4 shows the temperature drop from the moment the specimen heated to 800 °C was removed from the preheating oven; this was measured with a thermocouple buried in the specimen, as shown in Figure 2a. In this experiment, the compressive strength test was carried out within 4 min of removing the test specimen from the oven, and the temperature drop was confirmed to be 30 °C or less, except for the surface layer portion (A in Figure 4) and bottom (E in Figure 4) of the specimen within the range.

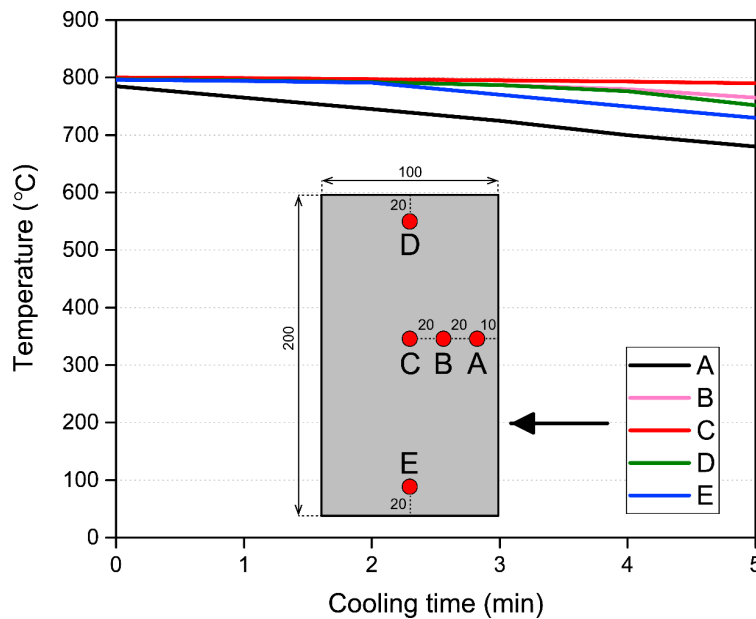


Figure 4. Temperature drop upon moving the oven-heated test specimen from the preheating oven to the compression tester (dimension unit of the specimen: mm). A–E: Location of thermocouples in the specimen.

In addition, for a comparison with the test method of the compressive strength during heating in the preheating oven proposed in this study, the validity of the test method was examined using the same level of test materials as those in the in situ-heating. In the comparative experiment, the compressive strength and elastic modulus were measured at 20, 200, 400, and 600 °C for the specimen with 10% EVA (E10, water content 2.0%) and without EVA (E0), at a heating rate of 100 °C/h. The test results are shown in Figure 5. For the mortar without EVA, the compressive strength and modulus of elasticity gradually decreased compared with the room temperature measurements. For E10, the strength decreased by approximately 50% when heating up to 200 °C. However, the strength and elastic modulus were partially restored when heating up to 400 °C. Furthermore, they decreased when heating up to 600 °C. Thus, regardless of the incorporation of EVA, both the heating methods (in situ- and oven-heating) showed a similar relationship. Therefore, the correlation between the test method using the preheating oven proposed in this study (oven-heating) and the existing hot test method (in situ-heating) was established. Based on the results, we concluded that the drop in temperature (up to 30 °C) when the sample was moved from the oven to the compression test apparatus did not have a significant effect on the test results. The results of the evaluation of the mechanical performance of the PCM specimens with various EVA incorporation ratios, using the oven-heating method proposed in this study, are described in more detail (Section 3.3).

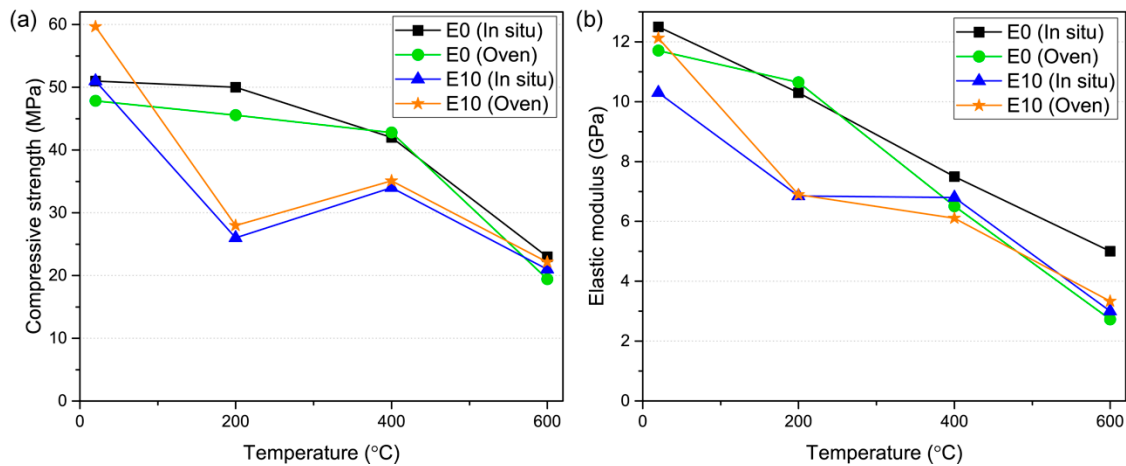


Figure 5. Comparison of (a) the compressive strength and (b) elastic modulus (in situ-heating vs. oven-heating).

3.3. Physical Properties of the PCM

Table 4 lists the air content and slump flow value for each combination of fresh PCM. As the polymer–cement ratio increased, the amount of air and slump flow increased. The increase in EVA content in PCM induced the increased water to cement mass ratio (W/C) of the PCM, resulting in higher air content and larger slump flow because EVA is intrinsically inert and acts as fine aggregates in the cement mortar. The increase in the number of air voids or pores in different scales owing to the incorporation of the polymer are discussed in detail with the MIP results (Section 4).

Table 4. Measurement results for the air content and slump flow of the PCM in fresh conditions.

Specimen	Polymer–Cement Ratio (P/C) (%)	Air Content (Average, %)	Slum Flow (mm)
E0	0	4.9	161 ± 10
E5	5	6.2	199 ± 8
E10	10	7.6	208 ± 9
E20	20	8.7	215 ± 7

The changes in the mass of the PCM specimens before and after heating are listed in Table 5. The mass loss ratios compared to the unheated specimen are also shown in Figure 6. The EVA-incorporated PCM specimens (E5, E10, and E15) exhibited a larger decrease in the mass loss ratio upon heating than those of E0. The higher the substitution ratio of EVA and the heating temperature were, the larger the decrease in the mass loss ratios became. Thus, E20 showed the highest mass loss ratio (approximately 13%) when heated to 800 °C, compared to the unheated specimen.

Table 5. Changes in the mass of the specimen before and after heating.

Type of PCM	Polymer-Cement Ratio (P/C) (%)	Heating Condition	Mass (g)				
			20 °C	200 °C	400 °C	600 °C	800 °C
E0	0	Before heating	417.0	412.7	414.3	415.5	410.4
		After heating	417.0	398.1	393.1	388.2	377.1
E5	5	Before heating	416.9	413.3	421.2	408.9	409.7
		After heating	416.9	394.8	396.3	379.9	373.3
E10	10	Before heating	412.5	414.1	412.0	410.2	409.9
		After heating	412.5	394.9	383.3	377.6	368.3
E20	20	Before heating	408.8	405.2	402.4	408.0	399.5
		After heating	408.8	384.5	371.2	370.9	353.0

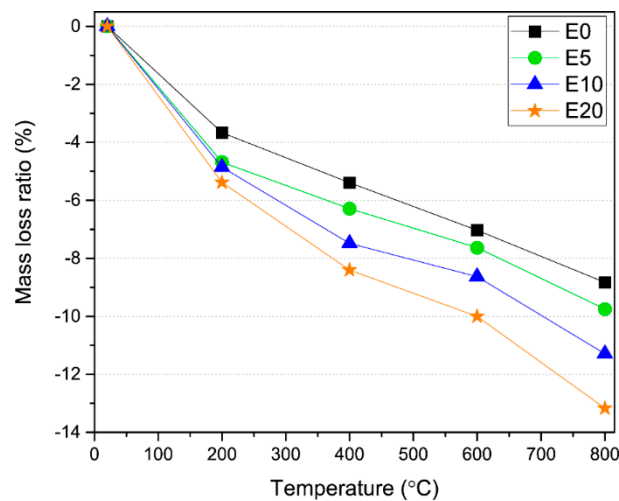


Figure 6. Mass loss of the PCM specimens owing to heating.

3.4. Mechanical Properties of the PCM Specimens Under Different Heating Conditions

Contents of the Cooling Specimen

Table 6 shows the compressive strength and modulus of elasticity change for the PCM specimens, depending on the heating temperature and conditions for cooling to room temperature after heating. Because the specimen had different initial values before heating, the ratios of residual compressive strength and elastic modulus were calculated as shown in Figure 7. The compressive strength gradually decreased by increasing heating temperatures. In the case of heating up to 600 °C and 800 °C, PCM exhibited similar compressive strength regardless of EVA contents. The elastic modulus also decreased

with the increase of EVA contents and heating temperature. In contrast to the compressive strength result, there is no significant degradation of elastic modulus when heated up to 200 °C.

Table 6. Compressive strength of the PCM specimens cooled after heating (100 × 200 mm) (in graph).

Temp. (°C)	Compressive Strength (MPa)				Elastic Modulus (GPa)			
	E0	E5	E10	E20	E0	E5	E10	E20
20	64.0	57.4	57.0	52.6	21.2	19.3	18.7	16.0
200	58.5	52.1	46.1	34.4	17.7	16.1	15.6	12.8
400	45.8	44.7	39.9	31.1	13.9	12.0	12.4	7.5
600	28.3	28.8	28.6	23.8	3.1	6.6	5.1	6.0
800	16.6	18.0	17.1	12.8	1.7	3.5	3.4	3.1

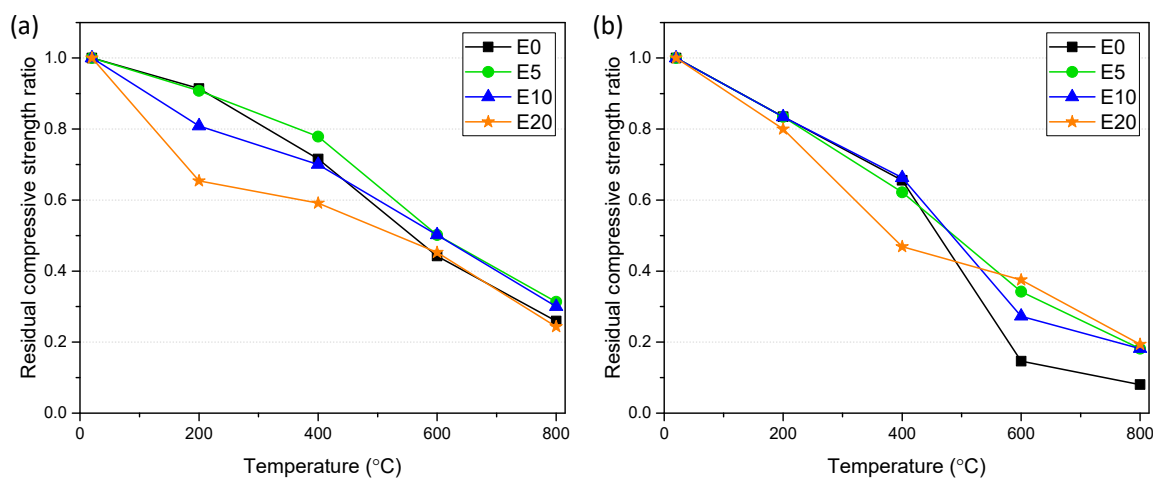


Figure 7. (a) The residual compressive strength ratio and (b) the residual elastic modulus ratio of the PCM specimens cooled after heating at different temperatures (200, 400, 600, and 800 °C).

Figure 8a depicts the compressive strength of the PCM specimens (E0, E5, E10, and E20) at each heating temperature (oven-heating). The residual compressive strength ratio of the heated PCM specimen compared to the unheated specimen is shown in Figure 7b. The degradation of the mechanical properties of the PCM specimens in a high-temperature environment was considered to be caused by the evaporation of the binding water, the thermal decomposition of the polymer, and the thermal decomposition of the hardened cement paste. The thermal properties of the bonded water and cement mortar and the deterioration of the mechanical properties of the mortar (or concrete) are listed in Table 7, based on the previous studies [14–17].

In this study, regardless of the heating conditions up to 200 °C, with an increase in the polymer–cement ratio, the compressive strength decreased sharply (Figure 8a) because the polymer melting point is from 70 to 120 °C which is very different trend compared to the results of cooling (see Figure 7). In the heating range of 200 to 400 °C, the compressive strength slightly recovered upon cooling, E10. Because of the residual strength ratio (Figure 8b), the strength decreased in proportion to the increase in the polymer–cement ratio, up to 400 °C; however, when heated to 600 °C and 800 °C, the residual strength ratio was approximately 0.4 and 0.3, respectively, regardless of the polymer–cement ratio. The decomposition of EVA dominated the deterioration of the mechanical properties of the PCM when heated up to 200 °C. However, the effect of the decomposition of C-S-H, which is the main hydration product of cement clinker, was dominant above 600 °C.

Table 7. Thermal properties of the hardened cement.

Temperature Section	Internal Reaction	Reaction Overview
~30–120 °C	Evaporation of physically adsorbed water	Water evaporation in large pores
~30–300 °C ~120–600 °C	Release of chemically adsorbed water; Gel tissue breakdown	Stepwise dehydration of $C_3A_3CSH_{32}$ C_3ACSH_{12} is dehydrated and forms (C_4A_3S) or CaO Dehydration of aluminite-based hydrates: C_3AH_6 Dehydrates at ~270–330 °C Completely dehydrates at 550 °C and forms $C_{12}A_7$ or CaO 160 °C: $CaSO_4 \cdot 2H_2O$ (Gypsum) \rightarrow $CaSO_4 + H_2O$ ~450–550 °C: $Ca(OH)_2 \rightarrow CaO + 2H_2O$
573 °C	Quartz phase change	Phase change $\alpha \rightarrow \beta$ -SiO ₂
~600–700 °C	C-S-H decomposition	β -C ₂ S formation
~580–920 °C	Calcium Carbonate (CaCO ₃) decomposition	Decomposition of limestone aggregate $CaCO_3 \rightarrow CaO + CO_2$
~1100–1200 °C	Concrete melting	Cement paste: melts around 1200 °C

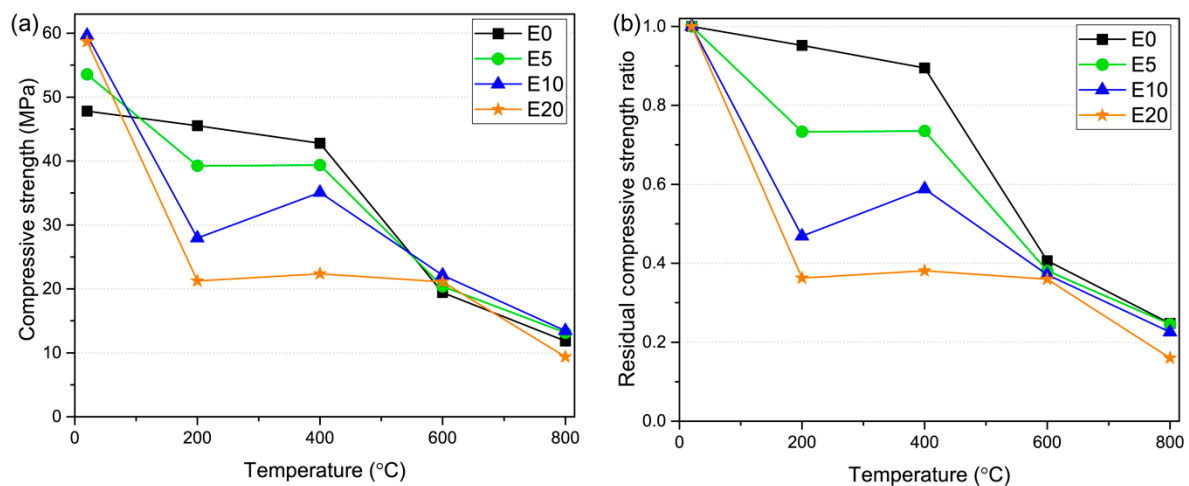


Figure 8. (a) Compressive strength of the PCM specimens heated at different temperatures (oven-heating, 200, 400, 600, and 800 °C) and (b) the residual compressive strength ratio compared to the unheated specimen.

Figure 9a shows the relationship between the moduli of elasticity of the PCM specimens at different heating temperatures, and Figure 9b shows the ratio of the modulus of elasticity at each heating temperature relative to the PCM at room temperature (unheated). The elastic modulus of the PCM decreased with an increase in the polymer–cement ratio. In the case of E10 and E20, the elastic modulus up to a heating temperature of 200 °C showed a sharp decrease as the polymer–cement ratio increased, as found in the compressive strength results. In addition, E10 and E20 exhibited a similar elastic modulus.

Figure 10 shows the stress–strain curve of the EVA-incorporated PCM at different heating temperatures (cooling). Before heating, more of the amount of EVA added a larger strain at the fracture of PCM was found. For all the PCMs, the strain at the fracture heated to 200 °C decreased, and when heated to 200 °C, the specimen became more brittle owing to the evaporation of free water. However, as the heating temperature increased, the strain value at the fracture point increased, indicating a more ductile characteristic. In E20, the ultimate strength and the strain at the time of fracture at 200 °C drastically decreased compared to E20 before heating; however, no significant difference was observed in the stress–strain curve compared to other PCM (E0, E5, and E10) at temperatures above 800 °C.

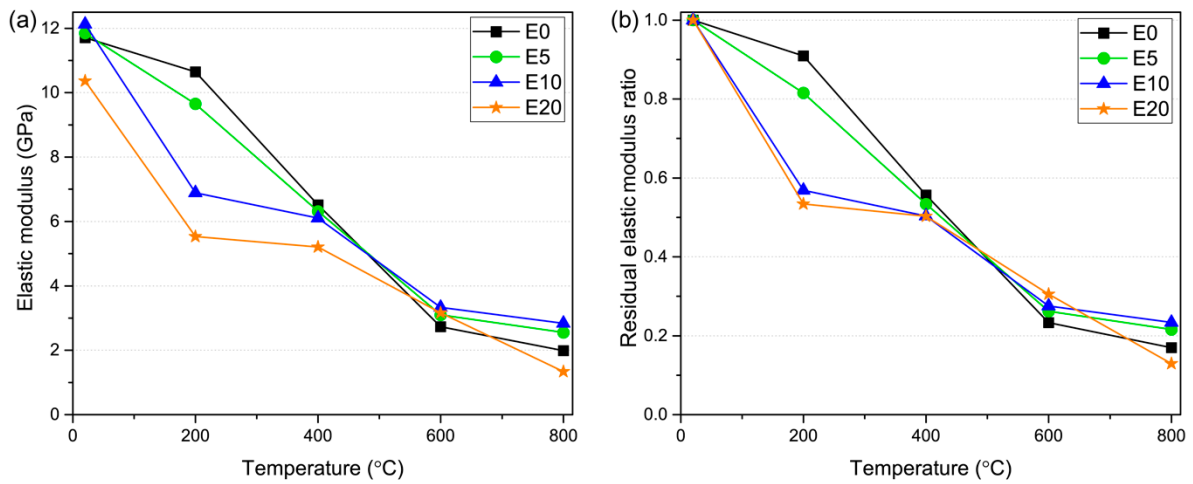


Figure 9. (a) Elastic modulus of the PCM specimens heated at different temperatures (oven-heating, 200, 400, 600, and 800 °C) and (b) the residual elastic modulus ratio of the PCM specimens compared to the unheated specimen.

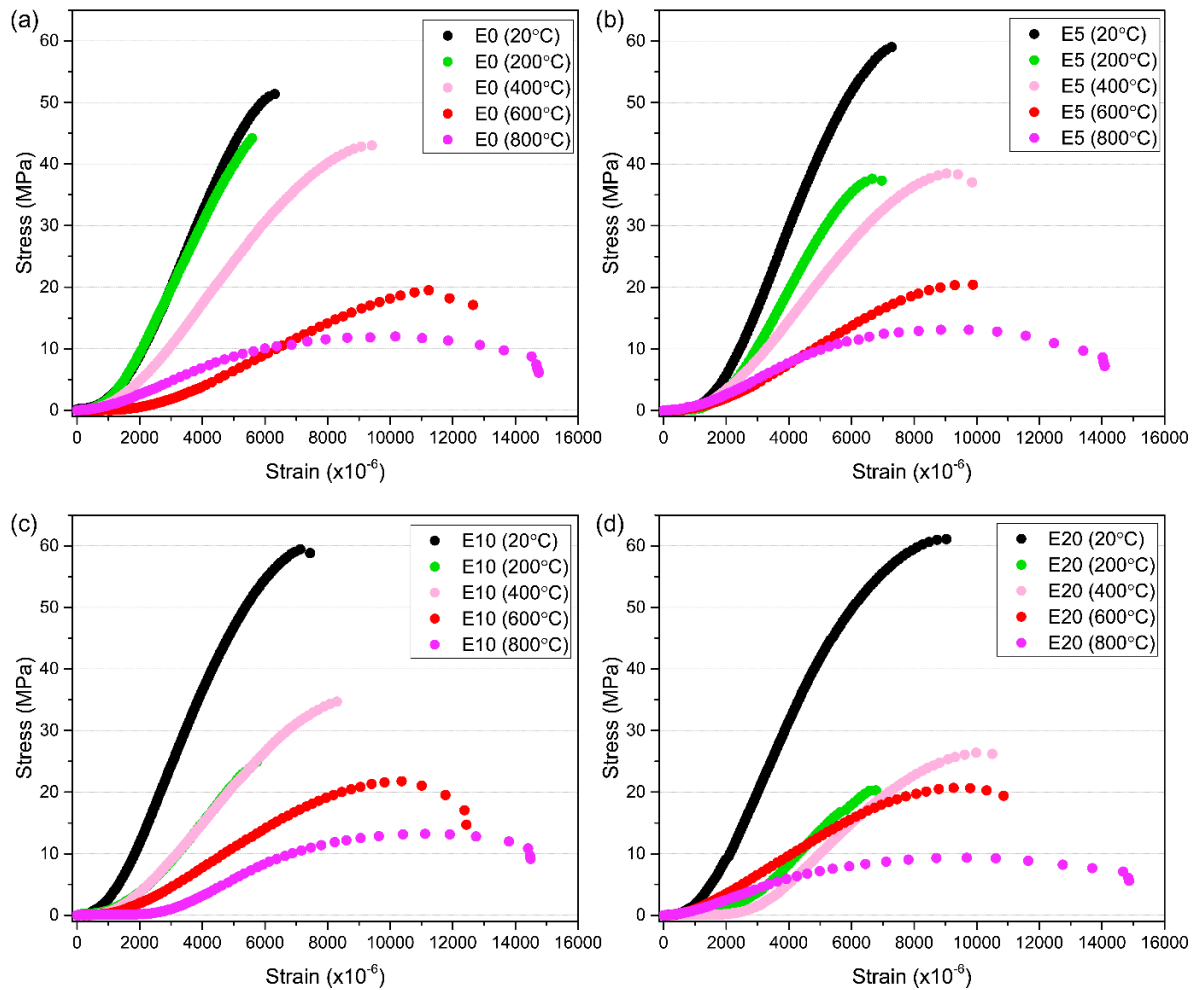


Figure 10. Stress–strain curve of the PCMs (a) E0, (b) E5, (c) E10, and (d) E20 heated at different temperatures.

3.5. Comparison of the PCM Mechanical Properties during Heating (In Situ- and Oven-Heating) and after Cooling

To confirm the mechanical properties of the PCM in a fire, a compression test under heating was conducted, and the compressive strength and elastic modulus were measured. In this study, a simpler heating method (oven-heating) was suggested and compared to the normal heating method (in situ-heating). In situ-heating of the PCM at high temperatures resembling a fire is more complicated than the compressive strength test for cooling after heating. For normal concrete, the strength (general strength and high strength) and residual ratio of the strength have been considered using different heating methods. However, for PCM, the residual ratio relationship of the specimen conditions (heating and cooling after heating) has not been considered.

Figure 11a,b shows the comparison of residual compressive strength and elastic modulus of the PCM, respectively, heated at different temperatures, depending on the mixing ratio of the EVA polymer and heating methods (oven-heating, and cooling). In the figure, the calculated values of the residual compressive strength and the elastic modulus of ordinary concrete without the polymer using a Eurocode [19] (in situ-heating) and Japanese code (JIS A 1171, cooling) are also shown. In the experimental results of the PCM using a cooling method, assuming that the PCM was cooled after a fire, the compressive strength ratio decreased gradually with the amount of incorporated polymer for all temperature ranges, which is similar to concrete followed by Euro and Japanese codes. However, the compressive strength ratio of the PCM in the oven-heating test showed sudden decreasing trends with the increase in the incorporation of the polymer, up to a temperature of 200 °C. The sudden change in compressive strength was assumed to be due to EVA decomposition in PCM which will be further discussed in the thermal analysis (see Section 4). The cooling process (from 200 °C to ambient temperature (20 °C)) was assumed to recover the cement paste matrix of the PCM. The residual modulus of elasticity also exhibited very similar trends to the results of compressive strength. It should be noted that the residual compressive strength ratio of the PCM converged to a similar value when heated up to 600 °C. In contrast, the residual elastic modulus ratio of PCM showed very similar values when heated up to 400 °C, which implies that the decomposition of the EVA affected the modulus of elasticity at lower temperatures.

Compared with the pyrolysis of the concrete properties shown as the Eurocode (in situ-heating) in Figure 11 [24], the mechanical properties of the PCM degraded with an increase in the polymer incorporation, although it varied slightly in the range of 200–400 °C. This was because of the evaporation of bound water in the mortar and the increase in the number of internal voids owing to polymer decomposition. At 600 °C and higher, the PCM strength remained constant, regardless of the amount of polymer and the heating method. At this temperature range, the decrease in strength was caused by the thermal decomposition of the cement paste material rather than the thermal decomposition of the polymer.

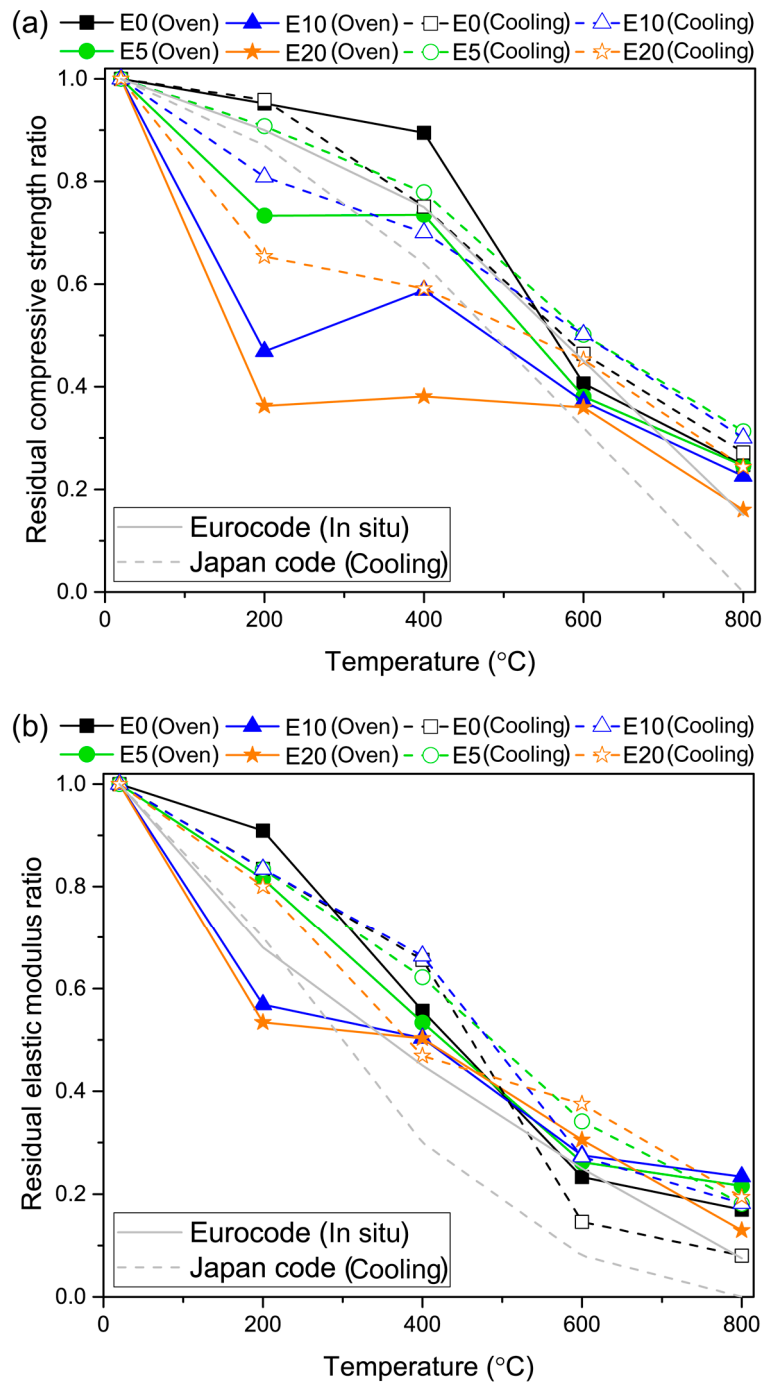


Figure 11. Changes in (a) the residual compressive strength ratio and (b) residual elastic modulus ratio of the PCM, depending on the heating method (in situ-heating, oven-heating, and cooling).

4. Thermogravimetric Results and Pore Structure of PCM Exposed to a High-Temperature

The mechanical properties of the PCM at high temperatures were experimentally confirmed by measuring the compressive strength and elastic modulus for each type and amount of polymer. The mechanical properties of the PCM specimens were different depending on the heating conditions (in situ-heating, oven-heating, and cooling). Furthermore, to investigate the PCM mechanical properties in the high-temperature region, in terms of the thermal decomposition of the polymer rather than the cement paste, the changes in mass, heat flow, and porosity were measured using TG, DSC, and MIP, respectively. Figure 12a depicts the mass change and heat flow of EVA. In the result of TG, there was a drastic mass reduction due to the decomposition of EVA (endothermic reaction) in the

temperature range from 280 °C to 400 °C. From 400 °C, exothermic heat flow was detected in EVA due to the combustion process. Approximately at 500 °C, all EVA was decomposed (100% mass reduction).

Figure 12b shows the change in the mass (TG) with the amount of incorporated polymer for the EVA-incorporated PCM. The mass change in the PCM confirmed that the higher the EVA substitution ratio, the greater the mass reduction owing to a temperature at 400 °C which was mostly caused by the thermal decomposition of EVA and the dehydration of cement hydrates as listed in Table 4. The decomposition of calcium hydroxide in the PCM was also observed between 400 and 500 °C. The mass loss above 600 °C was caused by the decomposition of carbonates and C–S–H [25,26].

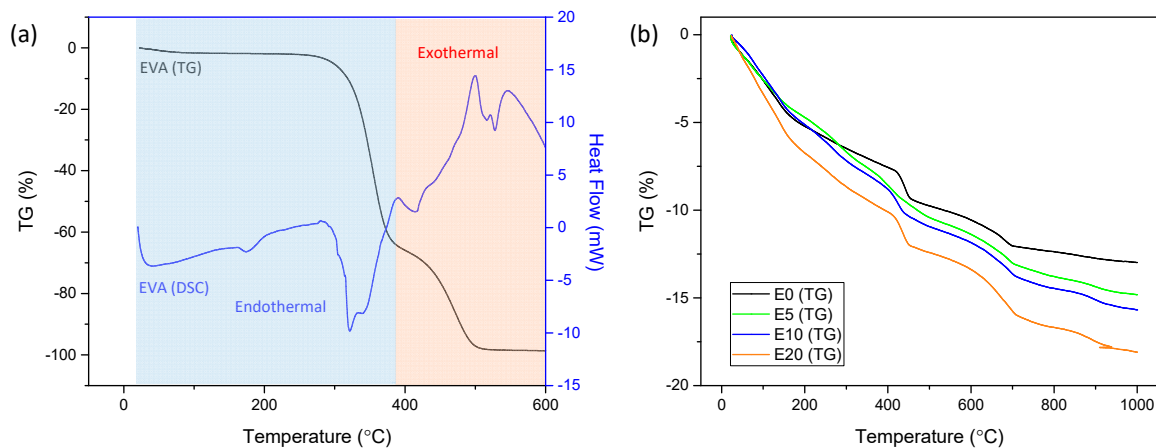


Figure 12. (a) Mass change (TG) and heat flow (DSC) for the EVA and (b) PCM based on the EVA content.

Figure 13 shows the change in the accumulated porosity (Figure 13a–d) and the distribution of the pores (Figure 13e–h) in the PCM mixed with EVA heated at different temperatures.

With an increase in the heating temperature, the pore size larger than 100 μm increased, and the increase was significant when heating to 600 °C. Except for E20, the porosity increased from 0.1 to 10 μm with an increase in the heating temperature.

Figure 14 shows the changes in the total porosity of the PCM depending on the EVA replacement rate with the heating temperature. Under the same heating temperature, the total porosity of the PCM increased as the EVA content increased. The total porosity of the PCM increased sharply at all levels when heating to 600 °C. This was because of the complete decomposition of calcium hydroxide in the cement paste and the initiation of the dissolution of carbonates and C–S–H. The porosity and pore diameter increased as the heating temperature increased, even at the same mixing ratio of EVA. Note that 600 °C was the critical temperature for the degradation of the elastic modulus. Therefore, the increase in the total pore and the pore structural changes had strong correlations with the elastic modulus of PCM.

In conclusion, the pore diameter and pore size of the PCM increased at each temperature range with an increase in the polymer incorporation ratio, and the total porosity increased from 19.1 to 30.8 vol.% for the EVA-free PCM and from 20.0, 21.0, and 23.6 vol.% to 35.1, 38.3, and 37.4 vol.% for the EVA-incorporated PCM when heating at 800 °C.

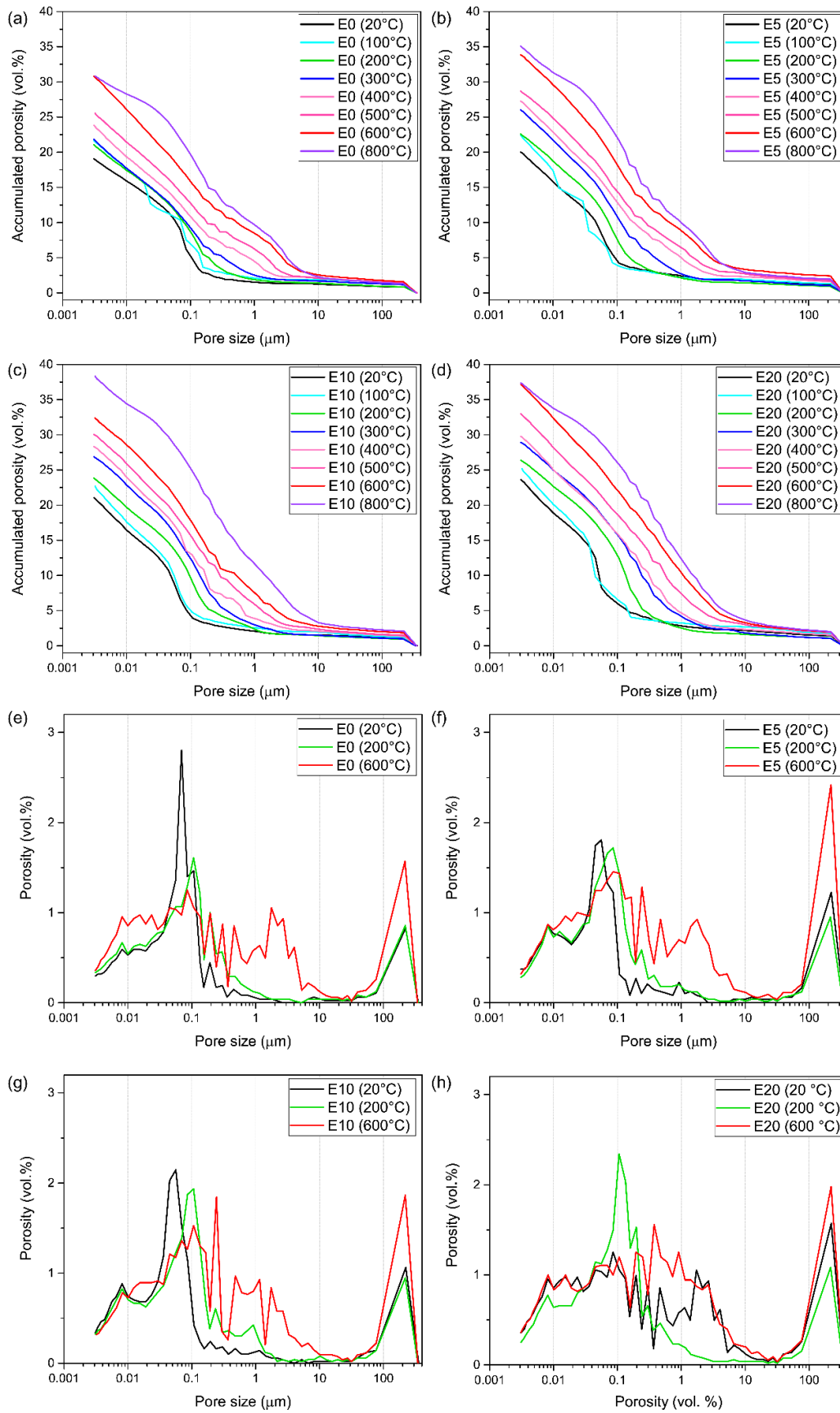


Figure 13. Changes in the porosity distribution and total accumulation porosity for the EVA incorporation amount and temperature range. (a–d) shows the accumulated porosity of E0, E5, E10, and E20, respectively. (e–h) shows the porosity distribution of E0, E5, E10, and E20, respectively.

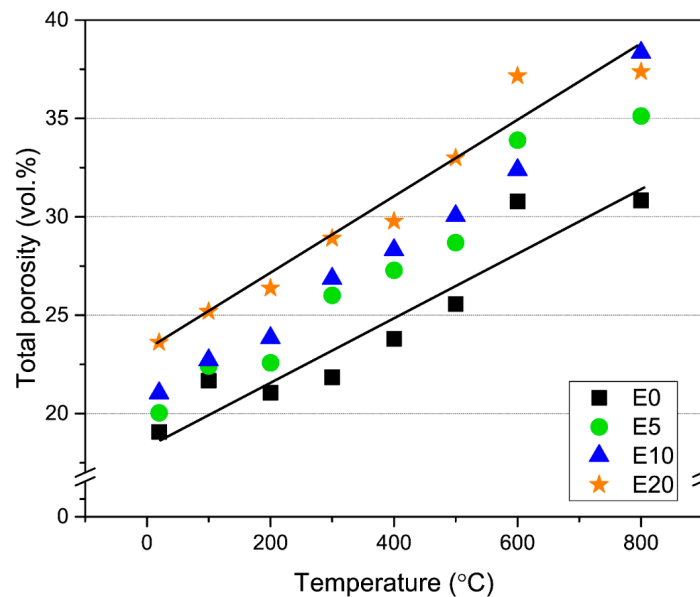


Figure 14. Comparison of the total accumulated porosity with the heating temperature and EVA replacement ratios.

5. Conclusions

In this study, the degradation in the mechanical properties of EVA-incorporated PCM, depending on the mixing ratio and heating temperature, was evaluated. The compressive strength and elastic modulus were measured in different heating conditions, and the characteristics of thermal decomposition and the change in the pore structure after heating were measured to analyze the correlation. The experimental results of this study are summarized as follows.

1. Regarding the mechanical properties of the PCM, the compressive strength and elastic modulus decreased when exposed to heating at different temperatures.
2. The compressive strength and elastic modulus of the PCM during heating at high temperatures significantly decreased when heated to 200 °C and 400 °C, respectively, regardless of the EVA mixing ratio. This was found to be because of the decomposition of EVA.
3. When the PCM was exposed to high temperatures, it was determined that the bonded water evaporated with an increase in the heating temperature, and simultaneously, the increase in the mass reduction and increase in the total amount of pores owing to the decomposition of the polymer and cement paste matrix decreased the mechanical performance of PCM.
4. For the amount of polymer admixture, there was a decrease in the mechanical properties at a polymer–cement ratio of 20% and a high temperature. When the polymer–cement ratio was 10% or less, a high residual ratio was observed.
5. The number of large pores and the total pore volume significantly increased with an increase in the polymer incorporation ratio. We also found that the decrease in the elastic modulus of the PCM at high temperatures was because of the increase in the number of pores, caused by the decomposition and the combustion of the polymer combined with the thermal decomposition of the cement paste.

Author Contributions: Investigation, H.-J.K., J.-Y.P. and B.-Y.C.; resources, H.-J.K.; visualization, J.-Y.P., H.-W.S. and S.-C.B.; Writing—Original Draft, H.-J.K. and S.-C.B.; Writing—Review and Editing, W.-J.P. and S.-C.B.

Funding: This research was funded by the National Fire Agency, “NEMA-Next Generation-2014-58”.

Acknowledgments: This research was supported by the Field-oriented Support of the Fire Fighting Technology Research and Development Program funded by the National Fire Agency (“NEMA-Next Generation-2014-58”).

Conflicts of Interest: The authors declare no conflict of interest.

References

1. Committee, A. State-of-the-art report on polymer modified concrete. *Am. Concr. Inst. ACI* **1995**, *548*, 1–47.
2. Sang, G.; Zhu, Y.; Yang, G. Mechanical properties of high porosity cement-based foam materials modified by EVA. *Constr. Build. Mater.* **2016**, *112*, 648–653. [[CrossRef](#)]
3. Wang, R.; Zhang, L. Mechanism and durability of repair systems in polymer-modified cement mortars. *Adv. Mater. Sci. Eng.* **2015**, *2015*, 594672. [[CrossRef](#)]
4. Yahia, A. Shear-thickening behavior of high-performance cement grouts—influencing mix-design parameters. *Cem. Concr. Res.* **2011**, *41*, 230–235. [[CrossRef](#)]
5. Yang, Y.; Yuan, B.; Sun, Q.; Tang, X.; Yingquan, X. Mechanical properties of EVA-modified cement for underground gas storage. *J. Nat. Gas Sci. Eng.* **2015**, *27*, 1846–1851. [[CrossRef](#)]
6. Zhang, Z.; Wang, P.; Wu, J. Dynamic mechanical properties of EVA polymer-modified cement paste at early age. *Phys. Procedia* **2012**, *25*, 305–310. [[CrossRef](#)]
7. Wang, M.; Wang, R.; Yao, H.; Farhan, S.; Zheng, S.; Wang, Z.; Du, C.; Jiang, H. Research on the mechanism of polymer latex modified cement. *Constr. Build. Mater.* **2016**, *111*, 710–718. [[CrossRef](#)]
8. Won, J.-P.; Choi, S.-W.; Park, C.-G.; Jang, C.-I. High strength polymer-modified repair cementitious composite for fire protection. *Polym. Polym. Compos.* **2007**, *15*, 379–388. [[CrossRef](#)]
9. Won, J.-P.; Kang, H.-B.; Lee, S.-J.; Kang, J.-W. Eco-friendly fireproof high-strength polymer cementitious composites. *Constr. Build. Mater.* **2012**, *30*, 406–412. [[CrossRef](#)]
10. Qiao, Y.; Deliwala, J.; Chakravarthula, S.; Kong, X. High-temperature tensile properties of a polymer intercalated/exfoliated cement. *Mater. Lett.* **2005**, *59*, 3616–3619. [[CrossRef](#)]
11. Hamasaki, H.J.K.; Noguchi, T. Study on heat release properties of polymer modified cement mortar. In Proceedings of the Part 1 Effect of the Unit Polymer Weight and Mixed Design, Annual Conference of Architectural Institute of Japan, Sendai, Japan, 26–29 August 2009; pp. 435–436.
12. Kim, H.H.; Noguchi, T. Study on heat release properties of polymer modified cement mortar. In Proceedings of the Part 2 Effect on the Thickness of Specimen on Annual Conference of Architectural Institute of Japan, Sendai, Japan, 26–29 August 2009; pp. 437–438.
13. Kim, H.-J.; Park, W.-J. Combustion and mechanical properties of polymer-modified cement mortar at high temperature. *Adv. Mater. Sci. Eng.* **2017**, *2017*. [[CrossRef](#)]
14. Bulletin 38. *Fire Design of Concrete Structures—Materials, Structures and Modelling*; Féd'eration Internationale du B'eton: Lausanne, Switzerland, 2007; p. 97.
15. Betioli, A.M.; Gleize, P.J.P.; John, V.M.; Pileggi, R.G. Effect of EVA on the fresh properties of cement paste. *Cem. Concr. Compos.* **2012**, *34*, 255–260. [[CrossRef](#)]
16. Mansur, A.A.; do Nascimento, O.L.; Mansur, H.S. Physico-chemical characterization of EVA-modified mortar and porcelain tiles interfaces. *Cem. Concr. Res.* **2009**, *39*, 1199–1208. [[CrossRef](#)]
17. Khoury, G.A. Compressive strength of concrete at high temperatures: A reassessment. *Mag. Concr. Res.* **1992**, *44*, 291–309. [[CrossRef](#)]
18. Medeiros, M.; Helene, P.; Selmo, S. Influence of EVA and acrylate polymers on some mechanical properties of cementitious repair mortars. *Constr. Build. Mater.* **2009**, *23*, 2527–2533. [[CrossRef](#)]
19. Eurocode 2: Design of Concrete Structures-Part 1-2: General Rules-Structural Fire Design. 2004. Available online: <https://www.phd.eng.br/wp-content/uploads/2015/12/en.1992.1.2.2004.pdf> (accessed on 5 May 2017).
20. Anagnostopoulos, C.A.; Sapidis, G.; Papastergiadis, E. Fundamental properties of epoxy resin-modified cement grouts. *Constr. Build. Mater.* **2016**, *125*, 184–195. [[CrossRef](#)]
21. J.S.A. *Loose Fill Thermal Insulation Materials*; Japanese Standards Association: Tokyo, Japan, 2016.
22. Park, D.; Ahn, J.; Oh, S.; Song, H.; Noguchi, T. Drying effect of polymer-modified cement for patch-repaired mortar on constraint stress. *Constr. Build. Mater.* **2009**, *23*, 434–447. [[CrossRef](#)]
23. Park, D.; Park, S.; Seo, Y.; Noguchi, T. Water absorption and constraint stress analysis of polymer-modified cement mortar used as a patch repair material. *Constr. Build. Mater.* **2012**, *28*, 819–830. [[CrossRef](#)]
24. Eurocode 4-Design of Composite Steel and Concrete Structure-Part 1-2: General Rules-Structural Fire Design. 1994. Available online: <https://www.phd.eng.br/wp-content/uploads/2015/12/en.1994.1.2.2005.pdf> (accessed on 5 May 2017).

25. ISO. *Reaction to Fire Tests for Building Products-non-Combustibility Test*; ISO: Geneva, Switzerland, 2010; Available online: https://infostore.saiglobal.com/preview/98701771998.pdf?sku=877775_SAIG_NSAI_NSAI_2086093 (accessed on 15 July 2017).
26. Reaction-to-Fire Tests–Heat Release, Smoke Production, and Mass Loss Rate–Part 1: Heat Release Rate (Cone Calorimeter Method) and Smoke Production Rate (Dynamic Measurement). Available online: <https://www.iso.org/standard/57957.html> (accessed on 15 July 2017).



© 2019 by the authors. Licensee MDPI, Basel, Switzerland. This article is an open access article distributed under the terms and conditions of the Creative Commons Attribution (CC BY) license (<http://creativecommons.org/licenses/by/4.0/>).